

Dense hydrogen plasma: Comparison between models

J. G. Clérouin and S. Bernard

CEA—Centre d'Etudes de Limeil-Valenton, 94195 Villeneuve St. Georges Cedex, France

(Received 30 September 1996; revised manuscript received 7 April 1997)

Static and dynamical properties of the dense hydrogen plasma ($\rho \geq 2.6 \text{ g cm}^{-3}$, $0.1 < T < 5 \text{ eV}$) in the strongly coupled regime are compared through different numerical approaches. It is shown that simplified density-functional molecular-dynamics simulations (DFMD), without orbitals, such as Thomas-Fermi Dirac or Thomas-Fermi-Dirac-Weiszäcker simulations give similar results to more sophisticated descriptions such as Car-Parrinello (CP), tight binding, or path-integral Monte Carlo, in a wide range of temperatures. At very low temperature, screening effects predicted by DFMD are still less pronounced than CP simulations. [S1063-651X(97)04709-0]

PACS number(s): 52.25.Kn, 02.70.Ns, 71.15.Pd, 71.10.-w

I. INTRODUCTION

In previous papers it has been shown that a simplified density-functional scheme adapted to plasmas [density-functional molecular dynamics (DFMD)] was able to reproduce accurately the equation of state of the hydrogen plasma at very high densities and in a wide range of temperatures [1,2]. The purpose of this paper is to present a more systematic comparison of static and dynamical properties of the dense hydrogen plasma between DFMD and other available models. The high-density regime can be characterized by a ratio $r_s = a/a_B$ [where $a = (4/3\pi\rho)^{-1/3}$ is the ion sphere radius, and a_B the Bohr radius] smaller or equal to unity. For such densities, the electronic orbitals of hydrogen are overlapping and electrons become delocalized [3]. This simple pressure ionization criterion can be checked by using the atomic physics package NOHEL [4] which predicts 80% of ionization, with a weak temperature dependence. More recent calculations have shown that this transition from high-pressure molecular hydrogen to the plasma phase occurs very abruptly through a first-order phase transition called the plasma phase transition [5], which can be located around $\rho = 1 \text{ g cm}^{-3}$ ending with a critical temperature of 15 000 K. Thus, for $r_s \leq 1$ ($\rho \geq 2.6 \text{ g cm}^{-3}$) the system can be considered as a strongly coupled fully ionized plasma.

It is clear that for lower densities ($r_s \geq 1.5$), a full quantum-mechanical treatment is needed to account for molecular binding. Techniques such as quantum Monte Carlo [6], density functional [7], or tight binding [8] are then necessary to investigate the pressure dissociation of molecular hydrogen. Conversely, for very high densities ($r_s \rightarrow 0$) where the electrons are fully degenerate ($\theta = T_e/T_F \rightarrow 0$, where T_F is the Fermi temperature) the electronic polarization becomes very weak and the system reduces to the one-component plasma (OCP).

In order to extract the dynamical behavior of the system (diffusion constant, viscosity), very long simulations with many ions are needed, and the accuracy of the physical model has to be balanced with computational cost. For example, the OCP model allows for simulations with 1000 ions over hundreds of plasma periods, but the lack of a good description of electron screening systematically underestimates the diffusion constant at finite r_s . Conversely, more

elaborate techniques based on the density matrix [9] are very accurate at lower densities (higher r_s) and finite temperature, but are limited to a few tens of ions. To treat the plasma regime, Car-Parrinello (CP) simulations have been pushed up to high densities [10,8], but limitations arise in describing electronic excited states. Moreover, the metallic character of the system induces a mixing between ionic and electronic degrees of freedom, leading to heat transfer between ions and electrons. In order to maintain the electronic density close to the Born-Oppenheimer surface, two Nose thermostats must be introduced to control electronic and ionic temperatures. At high temperature this procedure seems to induce a bias in the simulation, making conventional CP simulations almost impossible for temperatures $T > 1 \text{ eV}$. For higher temperatures, Kwon *et al.* proposed a tight-binding molecular-dynamics simulation [8] in which excited states are included in the Hamiltonian, allowing simulations up to a temperature of 5 eV.

By restraining our model to the plasma phase at $r_s \leq 1$, we can ignore all physical phenomena related to binding, and focus only on screening by finite-temperature electrons. The aim of this paper is to quantify the differences between DFMD models and the other models previously mentioned. The paper is organized as follows. In Sec. II we compare the concept of orbital free molecular dynamics with the classical Car-Parrinello scheme. Structural properties of the hydrogen plasma are then discussed depending on the model, and finally diffusion coefficients and collective modes are computed.

II. ORBITAL FREE FUNCTIONALS

In density-functional theory, the electronic energy is expressed as a sum of several terms: the kinetic energy E_{KE} , the Hartree energy E_{Hart} , the exchange-correlation energy E_{xc} , and external energy E_{ext} :

$$E[\rho] = E_{KE}[\rho] + E_{Hart}[\rho] + E_{xc}[\rho] + E_{ext}[\rho]. \quad (1)$$

The minimization of E depends only upon the electronic density $\rho(r)$ through the Hohenberg-Kohn (HK) theorem [11]. In the Kohn-Sham realization of the HK formalism, the electronic kinetic energy E_{KE} is calculated as the kinetic en-

ergy of a noninteracting electron gas, thus introducing a set of n_{occ} occupied electronic orbitals ψ_i :

$$E_{\text{KE}} = \sum_i \int dr \psi_i(r)^* (-\frac{1}{2}\nabla^2) \psi_i(r), \quad (2)$$

where the density is given by

$$\rho(r) = \sum_{i=1}^{n_{\text{occ}}} \psi_i(r)^* \psi_i(r). \quad (3)$$

The ψ_i 's are derived by solving the usual Kohn-Sham equations. In conventional CP molecular dynamics [12], the electronic degrees of freedom are these orbitals ψ_i (or more precisely the coefficients of their expansion on a set of plane waves) which are subject to an orthogonality constraint that represents a severe limitation to the size of the system.

A tempting alternative is to apply the HK theorem literally and to regard the electronic density $\rho(r)$ as the sole variable. One thus has to propose some functional form for the electronic kinetic energy as a function of the sole density (orbital free). Being the exact kinetic energy for a homogeneous system, the Thomas-Fermi (TF) theory appears to be the *paradigm* of such approximations. As a matter of fact, starting from the Thomas-Fermi expression $E_{\text{KE}} = c_0 \int \rho(r)^{5/3} dr$ with $c_0 = \frac{3}{10} (3\pi^2)^{2/3}$, a whole family of orbital free functionals have been developed. The first correction is to keep the TF kinetic energy and to add to the electronic Hartree term the exchange energy formula for the uniform electron gas computed by Dirac [Thomas-Fermi-Dirac (TFD) model]:

$$E_{\text{TFD}} = c_0 \int \rho(r)^{5/3} dr + c_x \int \rho(r)^{4/3} dr, \quad (4)$$

where $c_x = \frac{3}{4} (3/\pi)^{1/3}$. The next improvement is given by the addition of gradient corrections to the density:

$$E_{\text{KE}} = c_0 \int \rho(r)^{5/3} dr + \frac{\lambda}{8} \int \frac{|\nabla \rho(r)|^2}{\rho(r)} dr, \quad (5)$$

with a parameter $1 < \lambda < \frac{1}{9}$. The value of λ is a subject of great discussions and for isolated atoms energies calculations, the value $\frac{1}{2}$ seems to be the best [13]. Combined with the Dirac exchange term, this kinetic energy gives the Thomas-Fermi-Dirac-Weiszäcker (TFDW) functional.

More complex functionals have been devised, including the Lindhard response, or complex kernels, in order to reproduce some condensed matter features such as binding of atoms or total-energy calculations. Those functionals have been applied to sodium and aluminum [14–16], silicon [17–19], metal-salt solutions [20], clusters [21,18] and also hydrogen adsorbed on silicium surfaces [22].

But, keeping in mind that we are dealing with plasmas, some care must be taken in the choice of the kinetic-energy functional. However tempting it may seem to push the orbital free concept far enough to be able to reproduce some condensed-matter properties, it will probably give rise to more and more complex functionals, difficult to handle numerically and consequently computationally slower. Thus we have focused our comparison mostly on the TFD and TFDW

functionals which are easier to compute. Nevertheless, in addition to more complex calculations, the gradient term, when used at low densities, gives rise to negative densities. In this case a mass preconditioning must be introduced in order to control the pseudodynamics of each Fourier component of the electronic density [14].

Another advantage of dealing with Thomas-Fermi orbital free functionals is the possibility of performing finite electronic temperature calculations. The energy is then replaced by the free energy, also expressed locally as $F[\rho] = \int \mathcal{F}[\rho(r)] dr$, which acts as an effective potential for the ions. The extension of the Thomas-Fermi model to finite temperature was given by More [23] and Perrot [24] for the whole TFDW functional in the Kirzshnits formulation. Finite electronic temperature simulations are also possible with traditional Car-Parrinello simulations, but they require the implementation of a large set of excited states with occupation numbers f_i determined by the Fermi statistics through the use of the Mermin functional [9]. Finite electronic temperature simulations in quantum physics are now a very active field of research, where, due to their simplicity, orbital free functionals represent an interesting alternative.

III. COMPUTATIONAL DETAILS

Following the idea of Car and Parrinello, the dynamical evolution of the whole electron-ion system is controlled by a pseudo-Lagrangian, in which the density is the sole electronic dynamical variable. By taking the derivatives with respect to the density and ionic coordinates of the Lagrangian,

$$\mathcal{L} = \frac{1}{2} \mu \int \dot{\rho}^2(\mathbf{r}) d\mathbf{r} + \frac{1}{2} \sum_{i=1}^N M_i \dot{\mathbf{R}}_i^2 - F[\rho(\mathbf{r}), \mathbf{R}_i] - \mu \left(\int \rho(\mathbf{r}) d\mathbf{r} - N \right), \quad (6)$$

the equations of motion of both components are obtained. The only constraint here is charge neutrality, which is easily handled.

The external potential is given by the Coulomb potential, except for small distances ($r < r_c$), where it is regularized by an *ad hoc* homogeneous smearing of the nucleus leading to a parabolic core for the potential. We have checked [2] that, provided r_c stays smaller than a , this procedure yields no significant differences on collective properties compared with the bare Coulomb potential. However, this procedure precludes exact energy calculations, and a static correction must be introduced when calculating pressure [1].

By equating the ionic and electronic temperature, this scheme allows us to perform finite electron temperature simulations for 250 ions over $120\omega_p^{-1}$, where the plasma frequency is defined as $\omega_p = (3/M_I)^{1/2} r_s^{-3/2}$, in 10-h CPU of a YMP Cray computer. After an electronic minimization corresponding to the targeted electronic temperature, the ions are thermalized during $50\omega_p^{-1}$ by simple velocity rescaling. The simulation is then run without ionic and electronic thermostats. Total-energy conservation is better than one part in

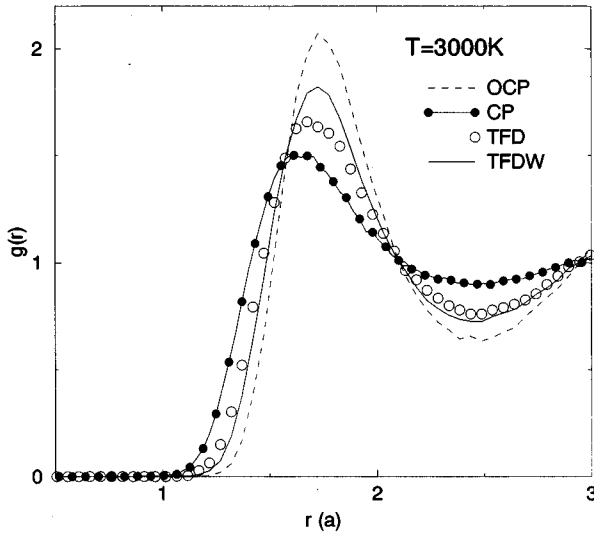


FIG. 1. Proton-proton pair distribution function for 3000 K and $r_s=1$. Long dashed curve is the OCP result; full curve with filled circles: Car-Parrinello simulations (CP); open circles: TFD simulations; full line: TFDW simulations.

10^4 , and the electron-ion mass ratio is adjusted to maintain the fake electronic energy lower than 10^{-3} times the ionic kinetic energy with no drift.

Simulations at the lowest temperature of 3000 K, corresponding to a plasma parameter $\Gamma = e^2/ak_B T = 104$, have been performed with the DFMD code using TFD and TFDW functionals and also with a CP code using BHS [25] pseudopotentials without thermostats (referred to as CP). To check our CP code, comparisons have been made with Kohanoff *et al.* CP simulations [10,26] using the bare Coulomb potential, without noticeable differences. Higher temperature runs ($T=5800, 7300, 11\,600, 29\,000$, and $58\,000$ K) corresponding to $\Gamma=50, 43, 27, 10$, and 5.4 have been done to compare with the tight-binding molecular-dynamics results of Kwon *et al.* [8].

IV. STRUCTURE

A structural comparison between DFMD's simulations and the other models [CP and path-integral Monte Carlo (PIMC)] at $r_s=1$, is provided by the computation of the proton-proton pair distribution function (pdf) $g(r)$ displayed in Figs. 1–3,

For the lowest temperature ($T=3000$ K and $\Gamma=104$, Fig. 1), the OCP model, in which interactions are unscreened, yields the most structured pdf, with the highest peak. Conversely, CP calculations give much less structure. The structures predicted by the DFMD models are intermediate between OCP and CP calculations. The first peak predicted by the TFD model is closer to the CP model than the one predicted by the TFDW model.

At higher temperature ($T=7300$ K and $\Gamma=43$, Fig. 2), the TFD and CP models are much closer, except for the first minimum which is more damped for CP calculations. The TFDW curve is still quite different.

At the highest temperature we considered ($T=29\,000$ K and $\Gamma=10$, Fig. 3), CP simulations are no longer reliable because of the drift in the fake energy, which is the sign of

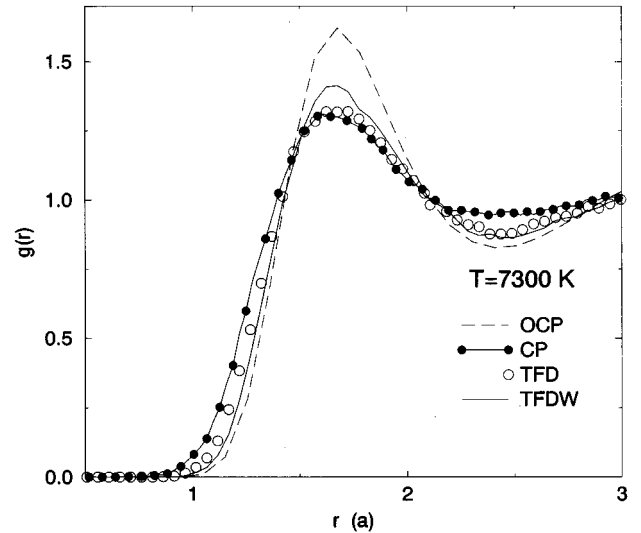


FIG. 2. Same as Fig. 1, for $T=7300$ K and $r_s=1$.

the loss of adiabaticity. The DFMD models must now be compared with the PIMC model [6], in which finite temperature electrons are described more accurately. The agreement is then very good, and the TFD curve is now very close to PIMC points. In particular, the closest approach distance is well reproduced, showing the importance of excited states on screening. Again, the TFDW model yields a slightly too high first peak.

V. INDIVIDUAL MOTION AND DIFFUSION

As shown in Ref. [27], the individual motions of atoms, revealed by the normalized velocity autocorrelation function

$$Z(t) = \frac{\langle v(t)v(0) \rangle}{\langle |v(0)|^2 \rangle},$$

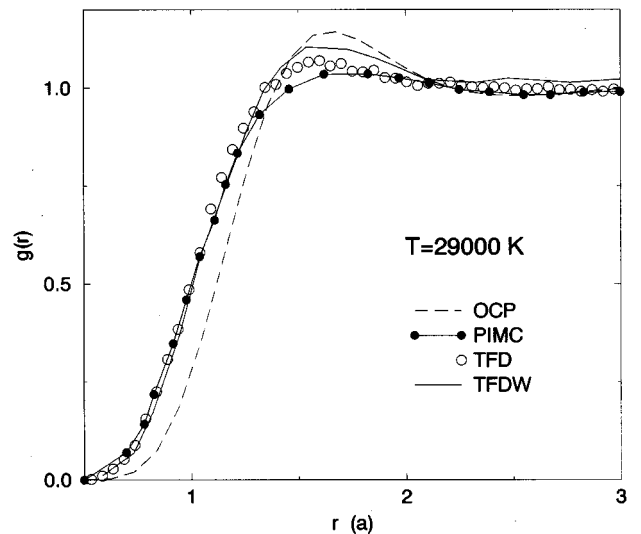


FIG. 3. Same as Fig. 1, for $T=29\,000$ K and $r_s=1$. Open circles are now for PIMC simulations.

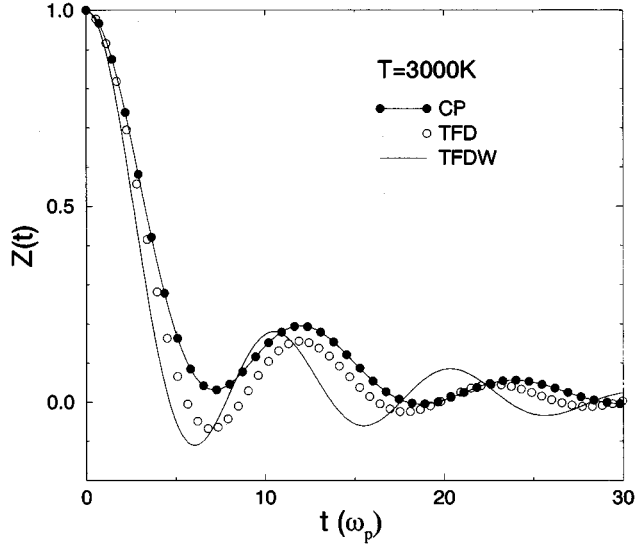


FIG. 4. Velocity autocorrelation functions for $T=3000$ K and $r_s=1$. Full curve with filled circles: Car-Parrinello simulations (CP); open circles: TFD simulations; and full line: TFDW simulations.

are dominated in the case of the OCP model by a long-lived plasma mode at a frequency close to ω_p . The same behavior is observed here, but with a characteristic frequency much lower than the plasma frequency. This lowering, first observed with simpler Thomas-Fermi simulations [2], also appears in CP simulations [26], and can be traced back to the reduced effective charge. In Fig. 4 we plot the normalized velocity autocorrelation function $Z(t)$ for $T=3000$ K at $r_s=1$. The OCP curve, which exhibits damped oscillations at a frequency close to ω_p (first maximum at the vicinity of $t=2\pi$) is not shown here for clarity. The basic period of damped oscillations of $Z(t)$ is now of the order of twice the OCP value for the CP simulations. This frequency is well reproduced by the TFD model, whereas the TFDW model predicts a lower frequency. At much higher temperature ($T=11600$ K) (Fig. 5), the convergence between CP and TFD becomes excellent, taking into account the uncertainties of CP simulations at high temperature, where adiabaticity is difficult to ensure.

From the time integration of the velocity autocorrelation function $Z(t)$, we have extracted the diffusion constant D in reduced units $a^2\omega_p$. Results using the DFMD models are compared with other models in Fig. 6 and Table I. We first plot the fit given in Ref. [27], $D=C\Gamma^{-\alpha}$, with $\alpha=-1.35$

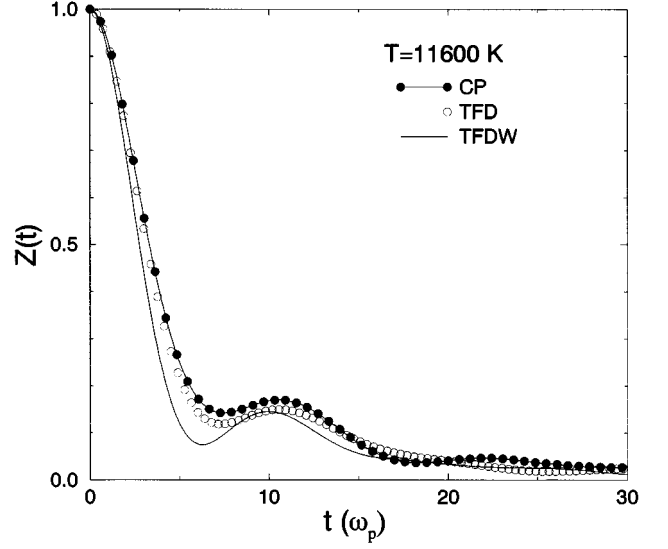


FIG. 5. Same as Fig. 3 for $T=11600$ K.

and $C=2.95$ for the OCP model, which yields a good estimation for low temperatures ($T<2$ eV) and provides a lower bound for diffusion. Some points from simulations of Ref. [27], and computed with our OCP code, are also plotted. At low temperature, CP computations of Kohanoff and Hansen using the bare Coulomb potential (referred in the figure as CPC) are reported together with our Car-Parrinello calculations with Pachelet-Hamann-Schlüter BHS pseudopotentials [25]. The agreement between the two calculations is fairly good at $\Gamma\approx 104$ ($T=3000$ K). For such a low temperature (3000 K) the diffusion constant calculated with the TFD model is 25% lower, but at higher temperature the TFD calculations are close to tight-binding (TB) values obtained by Kwon *et al.*, except for $\Gamma\approx 50$ where the TB value seems very high compared to the other models. Confirming the inspection of $g(r)$ and $Z(t)$, the TFDW functional yields poorer results. As previously mentioned by these authors, all estimations converge to the OCP value at high temperature.

VI. COLLECTIVE MODES

A more precise description of collective modes is provided by the computation of the charge-charge intermediate scattering function

$$F_{zz}(k,t) = \frac{1}{N} \langle \rho_z(k,t) \rho_z(-k,0) \rangle, \quad (7)$$

TABLE I. Diffusion coefficients vs coupling parameter Γ .

Γ	T (eV)	DFMD			Quantum	
		OCP	TFDW	TFD	TB	CP
104	0.26	0.006	0.010	0.012		0.016
50	0.5	0.015	0.025	0.033	0.043	0.030
43	0.63	0.020	0.031	0.037		0.038
27	1	0.038	0.054	0.068	0.072	0.067
10	2.5	0.134	0.164	0.192	0.186	
5.4	5	0.239	0.288	0.36	0.338	

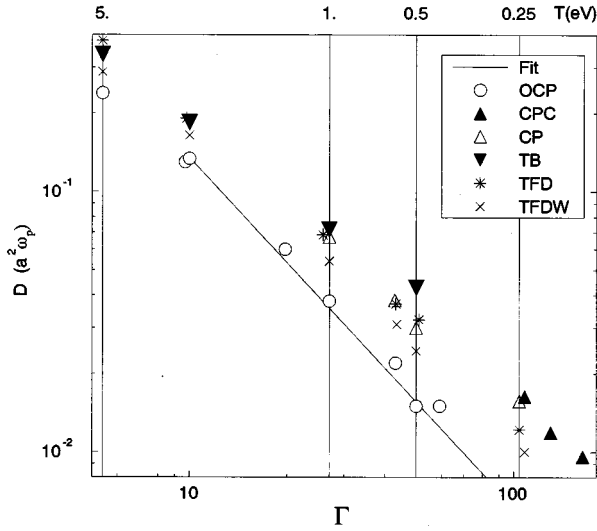


FIG. 6. Diffusion in units $a^2\omega_p$: The straight line is the fit given in Ref. [27] ($D=2.95\Gamma^{-1.34}$); open circles: OCP simulations; filled up triangles: Car and Parrinello simulations with Coulomb potential [10]; opened up triangles: Car and Parrinello simulations using BHS pseudopotentials; filled down triangles: tight-binding simulations [8]; stars: Thomas-Fermi Dirac simulations; crosses: Thomas-Fermi Dirac Weizsäcker simulations.

where $\rho_z(k,t) = \rho_i(k,t) - \rho_e(k,t)$, whose Fourier transform is the dynamical structure factor $S(k,\omega)$. Note that, due to the adiabatic motion of the electronic density, the charge-charge and proton-proton dynamical structure factors are very close, which would not be true if the system was treated as a fully dynamical ion-electron plasma. The screening has a dramatic effect in changing the low- k plasma modes. As pointed out by several authors [28], this screening is responsible for the appearance of an acoustic mode with a vanishing frequency in the $k \rightarrow 0$ limit, in contrast to the OCP model where the low- k limit is the plasma frequency ω_p . As shown in Fig. 7, TFD simulations reproduce this feature and our dispersion relation, computed by collecting the peak values of $S(k,\omega)$ and the half mean width, is very close to the one computed by Kohanoff and Hansen. The sound velocity c_s , given by the derivative of $S(k,\omega)$ with respect to k at the origin, is estimated from a fourth-order polynomial fit, and yields a value of $c_s \approx 40$ km/s. In order to compare with the Alavi-Parrinello-Frenkel estimation [29], we extrapolated their curve up to a pressure of 16 Mb, corresponding to $r_s = 1$. This extrapolation gives a sound velocity $c_s = 45 \pm 2$ km/s in good agreement with our result, corresponding to the upper range of pressures encountered on Jupiter [30].

VII. CONCLUSION

We have presented extensive comparisons of static and dynamical properties of hydrogen at high pressure (ρ

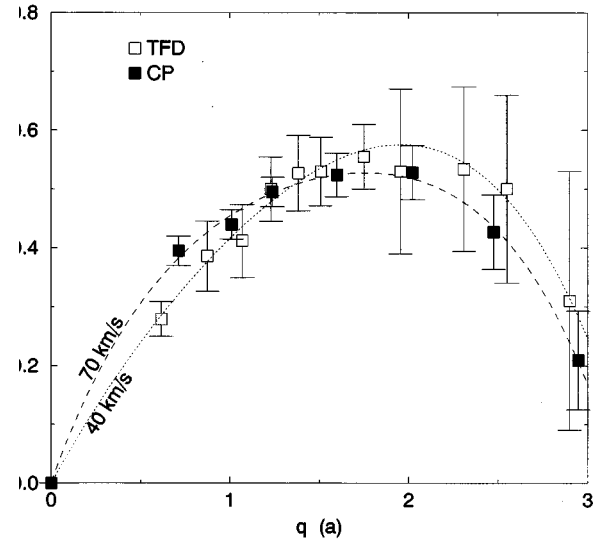


FIG. 7. Dispersion relation computed with the TFD model (open squares) and with the CP simulations of Kohanoff and Hansen (filled squares). Dotted (TFD) and dashed lines (CP) are fourth-order polynomial fits.

$= 2.6 \text{ g cm}^{-3}$) between very different models of increasing complexity. As expected, the OCP model appears as an asymptotic model and yields reasonable predictions for very high temperatures ($T > 5$ eV). The finite-temperature TFDW functional, which seemed the most accurate regarding total energies of isolated atoms [13], and which has proven to give a good equation of state for hydrogen (with some static correction) [1], gave somewhat disappointing results compared to the other models. Conversely, and surprisingly, the simpler TFD functional gives very good results for temperatures greater than 0.25 eV. Static and dynamical properties predicted by this model are in good agreement with Car-Parrinello, tight-binding and path-integral Monte Carlo calculations, with a much smaller computational effort. For such high temperatures, the TFD model appears to be easy to handle, in comparison with CP simulations where energy transfer between ions and electrons remains the main difficulty. However, at lower temperatures, where quantum effects are starting to come into play, the discrepancies with CP simulations are more important and call for a more accurate functional. For lower densities ($r_s > 1$), CP simulations appear undeniably necessary to take into account the formation of molecules. Thus the domain of validity of DFMD models can be limited by $\rho > 2.6 \text{ g cm}^{-3}$ (high-density region) and by $T > 0.3$ eV.

ACKNOWLEDGMENTS

The authors wish to acknowledge J. Kohanoff, B. Siberchicot, P. Dallot and J. P. Hansen for fruitful discussions.

- [1] J. I. Penman, J. Clérouin, and P. G. Zérah, Phys. Rev. E **51**, R5224 (1995).
 [2] J. Clérouin, E. L. Pollock, and P. G. Zérah, Phys. Rev. A **46**, 5130 (1992).

- [3] G. B. Zimmerman and R. M. More, J. Quantum. Spectrosc. Radiat. Transf. **23**, 517 (1980).
 [4] A. Decoster (unpublished).
 [5] D. Saumon and G. Chabrier, Phys. Rev. A **46**, 2084 (1992).

- [6] C. Pierleoni, D. M. Ceperley, B. Bernu, and W. R. Magro, Phys. Rev. Lett. **73**, 2145 (1994).
- [7] D. Holh, V. Natoli, D. M. Ceperley, and R. M. Martin, Phys. Rev. Lett. **71**, 541 (1993).
- [8] I. Kwon, L. A. Collins, J. D. Kress, N. Trouiller, and D. L. Lynch, Phys. Rev. E **49**, R4771 (1994).
- [9] A. Alavi, J. Kohanoff, M. Parrinello, and D. Frenkel, Phys. Rev. Lett. **73**, 2599 (1994).
- [10] Jorge Kohanoff and J. P. Hansen, Phys. Rev. Lett. **74**, 626 (1995).
- [11] P. Hohenberg and W. Kohn, Phys. Rev. B **136**, 864 (1964).
- [12] G. Galli and M. Parrinello, in *Computer Simulation in Material Science*, edited by M. Meyer and V. Pontikis (Kluwer, Dordrecht, 1991).
- [13] R. G. Parr and W. Wang, in *Density-Functional Theory of Atoms and Molecules* (Oxford University Press, Oxford, 1989).
- [14] M. Pearson, E. Smargiassi, and P. A. Madden, J. Phys. Condens. Matter **5**, 3221 (1993).
- [15] E. Smargiassi and P. A. Madden, Phys. Rev. B **49**, 5220 (1994).
- [16] M. Foley and P. A. Madden, Phys. Rev. B **53**, 10 589 (1996).
- [17] L. W. Wang, Ph.D. thesis, Cornell University, 1991.
- [18] N. Govind, J. L. Mozos, and H. Guo, Phys. Rev. B **51**, 7101 (1995).
- [19] L. W. Wang and M. T. Teter, Phys. Rev. B **45**, 13 196 (1992).
- [20] A. Meroni, J. P. Hansen, and P. A. Madden, J. Non-Cryst. Solids **156–158**, 771 (1993).
- [21] V. Shah, D. Nehete, and D. G. Kanhere, J. Phys. Condens. Matter **6**, 10 773 (1994).
- [22] N. Govind, J. Wang, and H. Guo, Phys. Rev. B **50**, 11 175 (1995).
- [23] R. M. More, Phys. Rev. A **19**, 1234 (1979).
- [24] F. Perrot, Phys. Rev. A **20**, 586 (1979).
- [25] D. R. Bachelet, M. Hamann, and G. B. Schlüter, Phys. Rev. B **26**, 4199 (1982).
- [26] Jorge Kohanoff and J. P. Hansen, Phys. Rev. E **54**, 768 (1996).
- [27] J. P. Hansen, I. R. Mc Donald, and E. L. Pollock, Phys. Rev. A **11**, 1025 (1975).
- [28] J. L. Barrat, J. P. Hansen, and H. Totsuji, J. Phys. C **21**, 4511 (1988).
- [29] A. Alavi, M. Parrinello, and D. Frenkel, Science **269**, 1252 (1995).
- [30] W. B. Hubbard, in *Simple Molecular Systems at Very High Density*, Vol. 186 of *NATO Advanced Study Institute Series B: Physics*, edited by A. Polian, P. Loubeyre, and N. Boccarra (Plenum, New York, 1989).